Role of Arg-72 of *pharaonis* Phoborhodopsin (Sensory Rhodopsin II) on its Photochemistry

Yukako Ikeura, Kazumi Shimono, Masayuki Iwamoto, Yuki Sudo, and Naoki Kamo
Laboratory of Biophysical Chemistry, Graduate School of Pharmaceutical Sciences, Hokkaido University, Sapporo, Japan

ABSTRACT *Pharaonis* phoborhodopsin (*p*pR, or *pharaonis* sensory rhodopsin II, NpsRII) is a sensor for the negative phototaxis of *Natronomonas* (*Natronobacterium*) *pharaonis*. Arginine 72 of *p*pR corresponds to Arg-82 of bacteriorhodopsin, which is a highly conserved residue among microbial rhodopsins. Using various Arg-72 *p*pR mutants, we obtained the following results: 1), Arg-72^{ppR} together possibly with Asp-193 influenced the pK_a of the counterion of the protonated Schiff base. 2), The M-rise became approximately four times faster than the wild-type. 3), Illumination causes proton uptake and release, and the pH profiles of the sequence of these two proton movements were different between R72A mutant and the wild-type; it is inferred that Arg-72 connects the proton transfer events occurring at both the Schiff base and an extracellular proton-releasing residue (Asp-193). 4), The M-decays of Arg-72 mutants were faster (~8–27 folds at pH 8 depending on mutants) than the wild-type, implying that the guanidinium prevents the proton transfer from the extracellular space to the deprotonated Schiff base. 5), The proton-pumping activities were decreased for mutants having increased M-decay rates, but the extent of the decrease was smaller than expected. The role of Arg-72 of *p*pR on the photochemistry was discussed.

INTRODUCTION

Halobacterium salinarum has four retinal membrane proteins: bacteriorhodopsin, i.e., bR (Oesterhelt and Stoeckenius, 1971; Lanyi and Luecke, 2001; Haupts et al., 1999); halorhodopsin, i.e., hR (Varo, 2000; Mukohata et al., 1999); sensory rhodopsin, i.e., sR or sRI (Hoff et al., 1997); and phoborhodopsin, i.e., pR; also called sensory rhodopsin II, or sRII (Kamo et al., 2001; Sasaki and Spudich, 2000; Takahashi et al., 1985). The first two work as light-driven ion pumps—bR as an outward proton pump, and hR as an inward Cl^- pump. The second two work as photosensors that relay light signals to their cognate transducer proteins, which initiates a phosphorylation cascade that regulates the flagella motors to control phototaxis. The ground state of sRI (absorption maximum, i.e., λ_{max}, is equal to 587 nm) mediates positive phototaxis whereas its long-lived photointermediate (λ_{max} = 373 nm) is a sensor for negative phototaxis (Spudich and Bogomolni, 1984). Phoborhodopsin or sRII (λ_{max} = 480 nm) is also a sensor for negative phototaxis (Takahashi et al., 1985). Thus, this bacterium is attracted toward light longer than 520 nm where the two ion pumps can work (Tomioka et al., 1986), and repelled from the shorter wavelength light that contains harmful UV light. *Pharaonis* phoborhodopsin (*p*pR) or *pharaonis* sensory rhodopsin II (NpsRII) is a photosensor in *Natronomonas* (*Natronobacterium*) *pharaonis* corresponding to pR (or sRII) of *H. salinarum* (Hirayama et al., 1992; Lüttenberg et al., 1998). *p*pR (NpsRII) is more stable than pR (sRII), especially in dilute salt solutions (Scharf et al., 1992). Success in the functional expression of *p*pR in *Escherichia coli* cell membranes allowed a simple preparation of the protein in large amounts, which permitted more detailed investigations (Shimono et al., 1997).

The amino acid sequence has been determined for all four kinds of pigments, and the sequences aligned (Zhang et al., 1999; Shimono et al., 1998; Ihara et al., 1999). Three-dimensional structures are now available for all archaeal rhodopsins with the exception of sRI: the structure of bR was reviewed by Lanyi and Luecke (2001) and Neutze et al. (2002); hR was by Kolbe et al. (2000); and NpsRII (or *p*pR) was by two groups, Luecke et al. (2001) and Royant et al (2001). The general features of the structure are quite similar with seven transmembrane helices (A–G) situated almost perpendicular to the membrane. The chromophore (all-*trans*-retinal) binds to a lysine residue located on helix G via a protonated Schiff base. The structures of the membrane helices of *p*pR and bR are very similar to each other; the root mean-square deviation value between bR and *p*pR is 0.95 Å^2 when the transmembrane helices are confined, and this value is reduced to 0.77 Å^2 with only C–G helices being confined (Pebay-Peyroula et al., 2002). On excitation by light, the chromophore of each of these four pigments undergoes an all-*trans* → 13-*cis* isomerization (Imamoto et al., 1992a), which is followed by thermal relaxations to the original state through a set of photochemical intermediates (Miyazaki et al., 1992; Chizhov et al., 1998). This sequence is called *photocycling*. Differences between ion-pumping and photosensor rhodopsins are that 1), the photocycling rate of the photosensor is much slower (seconds) than that of the ion pumps (~10 ms) (Imamoto et al., 1992b; Scharf et al., 1992), and 2), the photosensor of sR and pR is associated with

Submitted September 15, 2003, and accepted for publication December 12, 2003.

Address reprint requests to Naoki Kamo, Tel.: 81-11-706-3923; Fax: 81-11-706-4984; E-mail: nkamo@pharm.hokudai.ac.jp.

Abbreviations used: bR, bacteriorhodopsin; hR, halorhodopsin; sR, sensory rhodopsin; pR, phoborhodopsin; *p*pR, *pharaonis* phoborhodopsin (sensory rhodopsin II); NpsRII, *pharaonis* sensory rhodopsin II; *p*HtrII, halobacterial transducer for *pharaonis* phoborhodopsin (sensory rhodopsin II); Arg-82^{bR}, arginine residue at 82nd position of bR; Arg-72^{ppR}, arginine residue at 72nd position of *p*pR; EC, extracellular channel; CP, cytoplasmic channel; R72A^{ppR}, mutant in which Arg-72^{ppR} is replaced with Ala.

0006-3495/04/05/3112/09 $2.00

a cognate transducer within the membrane called HtrI and HtrII (*p*HtrII for *p*pR), respectively (Yao and Spudich, 1992, 2001; Hoff et al., 1997; Spudich, 1998; Zhang et al., 1999). The x-ray structure of the complex between NpsRII (*p*pR) and its truncated *p*HtrII was solved by Gordeliy et al. (2002).

Alignment of primary amino acid sequences identifies Arg-82^{bR} or Arg-72^{ppR} as a highly conserved residue among archaeal rhodopsins (Ihara et al., 1999; Spudich et al., 2000; Brown, 2001), and hence this residue is considered a very important residue. This Arg residue is also found in proteorhodopsin from sea bacteria (Beja et al., 2001), NOP-1 from *Neurospore crassa* (Bieszke et al., 1999), *Chlamydomonas reinhardtii* sensory rhodopsin (Sineshchekov et al., 2002), and *Anabaena* sensory rhodopsins (Jung et al., 2003). The role of Arg-82^{bR} has been investigated in bR: this residue controls the proton release to the extracellular space; the pK_a value of Asp-85^{bR} that is a counterion of the protonated Schiff base; and the rate of retinal thermal isomerization (Balashov et al., 1993; 1995; Govindjee et al., 1996).

The crystal structure of *p*pR (NpsRII) shows that the guanidinium group of Arg-72^{ppR} is oriented toward the extracellular side of the membrane compared to that of Arg-82^{bR} (Luecke et al., 2001; Royant et al., 2002), meaning that the distance of each guanidinium nitrogen atom of Arg-72 from the Schiff base is ~11 Å, whereas the distance of that in bR is ~8 Å. This difference is considered to cause the interaction between Arg-72^{ppR} and Asp-75^{ppR}, as counterion of the protonated Schiff base, to become weak in comparison with that in bR. This difference may give rise to pK_a differences of functionally important amino acids of *p*pR from those of bR.

The aim of this article is to clarify the role of Arg-72^{ppR} on the photochemistry of *p*pR, and for this end, we investigated the photocycling and the proton transport of various Arg-72^{ppR} mutants. The M-decays of Arg-72^{ppR} mutants were faster (~8–27 folds at pH 8, depending on mutants) than the wild-type, which is interpreted as the positive charge of the guanidinium preventing the proton transfer through the extracellular channel (EC) to the unprotonated Schiff base during M-decay. In addition, this Arg-72^{ppR} controls the pK_a value of Asp-75^{ppR}, the counterion of the protonated Schiff base. The timing of the light-induced proton release and uptake of Arg-72^{ppR} was found to be different from that of the wild-type. The preliminary results were presented at the 1st Asian Conference on Photobiology at Awaji Island, Hyogo, Japan (Ikeura et al., 2002).

MATERIALS AND METHODS

Preparation of samples

Expression and purification of histidine-tagged recombinant *p*pR and Arg-72^{ppR} mutant proteins were essentially the same as described previously (Ikeura et al., 2003; Shimono et al., 1997). The proteins were reconstituted with L-α-phosphatidylcholine (PC from egg, Avanti, Alabaster, AL) with the molar ratio of 1:50, and the procedure was the same as described previously (Iwamoto et al., 2003; Kandori et al., 2001).

pH titration

Proteins reconstituted with egg-PC were suspended in 400 mM NaCl supplemented with six-mixed buffer (citric acid, MES, HEPES, MOPS, CHES, and CAPS, each at 10-mM concentration). After washing 2 or 3 times (15,000 × *g* for 30 min) the sample was resuspended. This six-mixed buffer has the advantage of an approximately constant buffer strength over a wide pH range (Balashov et al., 1995). The spectra at varying pHs were obtained using a U-3210 spectrophotometer (Hitachi, Tokyo, Japan) in which an end-on photomultiplier was installed to reduce the scattering artifact. The pH was adjusted to the desired value using H_2SO_4 or NaOH. Temperature was 20°C. Data were analyzed with a model of two interacting residues (Balashov et al., 1995) and data fitting was done using Microcal Origin software (Microcal Software, Northampton, MA).

Flash-photolysis measurements

For measurements in the time range longer than milliseconds (such as M-decay, O-decay, and the recovery of the original pigment), a Xe-flash (>540 nm, 200 μs of the duration) was used with an appropriate combination of filters (KL54/Y52, Toshiba, Tokyo, Japan). The apparatus and methods were the same as those described previously in Miyazaki et al. (1992). For the measurement of M-rise, the second harmonic of the fundamental beam of the Q-switched ND-YAG laser (532 nm, 7 ns) was employed as an actinic-light source, and data were accumulated 100 times for each run.

Light-induced proton transfer (release or uptake)

The egg-PC-reconstituted samples were washed two or three times and suspended in pure water. Fifty to one hundred microliters of this suspension (~10 μM of *p*pR) was dropped on a transparent SnO_2 electrode surface and dried (diameter of spot, ~10 mm). The adhesion was so strong that the protein was not detached from the electrode surface unless washed with a detergent. This has been inferred from the fact that repeated use of the electrode is possible without any change in the signal amplitude. This SnO_2 electrode was used as a working electrode and another SnO_2 electrode was used as a counterelectrode. A solution of 400 mM NaCl was sandwiched by these two electrodes, and the solution was supplemented with 1 mM of the six-mixed buffer, the pH of which was adjusted with H_2SO_4 or NaOH to the desired value. An electronic circuit was used that was essentially the same as previously described in Iwamoto et al. (1999a). The light-generated electromotive force that arose between the two SnO_2 electrodes was picked up and amplified through a 15-Hz low-cut filter (MEG-1200, Nihon-Koden, Tokyo, Japan). This filter eliminated signals due to the fluctuation of the baseline and differentiated the signals. The actinic-light pulse (duration of 4 ms) was provided by a mechanical shutter as described elsewhere (Iwamoto et al., 2003).

Light-induced proton transport

Photoinduced proton transport by the wild-type *p*pR or Arg-72^{ppR} mutants was assayed using inside-out membrane vesicles that were prepared by passing the cells through a French press (500–700 kg/cm^2, Ohtake, Tokyo, Japan) (Ikeura et al., 2002; Sudo et al., 2001). The photoinduced pH change in the vesicle suspension was measured with a SnO_2 electrode. One hundred microliters of the vesicle suspension was confined on the surface of the SnO_2 electrode using a dialysis membrane. The amounts of *p*pR or mutants in this vesicle suspension were adjusted to be constant at 66 μg. The other surface of this dialysis membrane is faced to 400 mM NaCl without buffer, with which another SnO_2 electrode as a counterelectrode was contacted. Electric

signals arising between a pair of SnO_2 electrodes were measured with a DC potentiometer (Potentiostat/Galvanostat 2000, Toho Technical Research, Naruse, Machida, Japan). The constant actinic light was provided from 300 W Xe-lamp through a hot mirror, an interference filter (500 nm), and a cutoff filter (Y46 > 460 nm).

RESULTS

pK_a of the counterion of the Schiff base

The pK_a of the counterion of the Schiff base, Asp-75^{ppR}, can be estimated by pH titration: when it is protonated, the maximum wavelength is red-shifted, and the color turns to pink (Chizhov et al., 1998; Shimono et al., 2000). The titration data are plotted in Fig. 1, where the ordinate represents the ratio of A_{541} at the respective pH to that at a sufficiently low pH where all the pigment is in the pink form. This ratio represents the fraction of the pink form. This figure shows that the order of the pK_a is wild-type < R72K < R72A < R72Q, revealing that Arg-72^{ppR}, presumably due to the positive charge of guanidinium group, decreases the pK_a of the counterion.

The titration curves were analyzed with the Henderson-Hasselbalch equation, and it was found that data were well fitted with an equation with a single pK_a for R72A^{ppR} and R72Q^{ppR} in which Arg-72^{ppR} was replaced with a neutral amino acid. In contrast, for the mutant containing a positively charged residue (R72K^{ppR}) as well as for the wild-type, the data cannot be fitted with a single pK_a equation but could be successfully fit using the schema described in an inset of Fig. 1. This scheme implies that the pK_a of the counterion is affected by the ionization state of another residue (*X*)

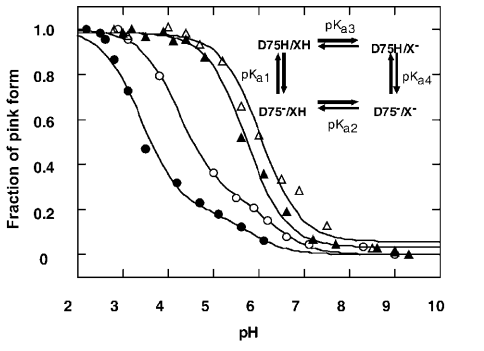

		pK_{a1}	pK_{a2}	pK_{a3}	pK_{a4}
●	Wild-type	3.5	5.7	4.1	5.1
▲	R72A	5.7			
○	R72K	4.4	6.2	4.8	5.7
△	R72Q	6.0			

FIGURE 1 Spectroscopic pH titration to determine pK_a of Asp-75^{ppR}, the counterion of the protonated Schiff base. The ordinate represents the ratio of the 541-nm absorbance at the respective pH (see text). The protein (~10 μM) was suspended in 400 mM NaCl supplemented with six-mixed buffer (see Materials and Methods), and the pH was adjusted with H_2SO_4 or NaOH. The titration data were analyzed with the scheme shown in the inset and pK_a values were estimated with a nonlinear regression. Temperature was 20°C.

(compare pK_{a1} and pK_{a4}), and the pK_a of *X* is, in turn, affected by the ionization state of Asp-75^{ppR}, the counterion (compare pK_{a3} and pK_{a4}) (Balashov et al., 1995).

The pK_a values of wild-type determined here are different from those previously reported (Chizhov et al., 1998; Shimono et al., 2000), but our recent results (Mizuta et al., unpublished results) show the large dependence on lipid species used.

The pK_a of the protonated Schiff base may be changed by the replacement of Arg-72^{ppR}. Unfortunately, however, the exact value cannot be determined, but seems to be a little larger than that of the wild-type in the dark (>12; S. P. Balashov, unpublished results).

Proton release or uptake at an earlier stage of the photocycling

During the photocycling of *p*pR, proton release and uptake occur (Iwamoto et al., 1999a). Fig. 2 *A* shows light-induced proton transfer for the wild-type (400 mM NaCl, pH 5.0). Note that the signal has been differentiated with a 15-Hz low-cut filter. The positive signal indicates proton release from *p*pR. This figure reveals that the proton release occurs first when illumination was applied, followed by the uptake. This observation is different from that reported previously (Iwamoto et al., 1999a). We note that the present sample is reconstituted with egg-PC, and that for solubilized *p*pR, proton uptake and release coincide with the O-formation and O-decay, respectively, as was reported previously (Iwamoto et al., 1999a). R72Q^{ppR} shows first proton uptake followed by release, as shown in Fig. 2 *B*. The medium contained 400 mM NaCl at pH 8.0.

In Fig. 2, *C* and *D*, the magnitudes of the first events observed immediately after the light stimuli are plotted against the pH of the medium. The wild-type (Fig. 2 *C*) and R72A^{ppR} (Fig. 2 *D*) data are quite different: the mutant never shows positive values, meaning that proton uptake precedes release over the whole pH range examined. The results for R72Q^{ppR} were the same as R72A^{ppR} (data not shown). In contrast, the wild-type shows positive (pH ~3–7) and negative (pH ~7–10) signals. This figure clearly shows that the Arg-72^{ppR} affects the timing of the proton release, similar to the effected Arg-82^{bR} (Balashov et al., 1993; Govindjee et al., 1996).

Effect on the rise of M-intermediate

The rise of M-intermediate was measured after a laser flash: in the presence of 400 mM NaCl (pH 8.0), this process was analyzed well by a single exponential equation and the time constants observed were 0.05 and 0.22 μs^{-1} for the wild-type and R72A^{ppR}, respectively. The rate for the mutant is approximately four times larger than that of the wild-type. The disappearance of the positive charge of guanidinium facilitates proton transfer from the Schiff base to the

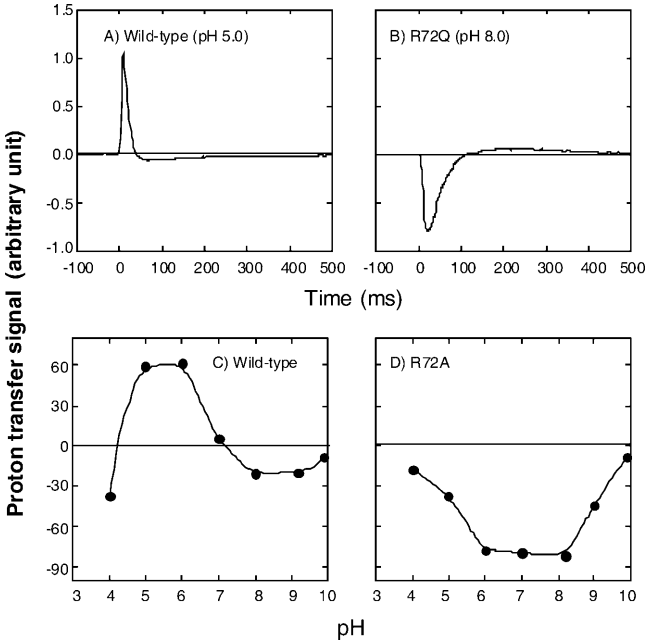

FIGURE 2 Flash-induced proton transfer reaction of the wild-type (*A* and *C*) and Arg-72^{ppR} mutant (*B* and *D*). R72Q was used in *B* and R72A was used in *D*. *A* and *B* show the proton transfer data measured by SnO_2 electrode. The potential difference between a pair of SnO_2 electrodes was measured using a 15-Hz low-cut filter, which gave the differentiated signals. For the wild-type (*A*), the light pulse (4-ms duration) led first to proton release, followed by the uptake. *B* shows the opposite sequence for R72Q^{ppR}. The magnitudes of the first photoresponses are plotted against pH in *C* and *D* for the wild-type and R72A^{ppR}. The medium for all experiments was 400 mM NaCl. The pH values in *A* and *B* were 5.0 and 8.0, respectively. For detailed experimental procedures, see Materials and Methods.

deprotonated counterion, Asp-75^{ppR}. Similar increases in the M-rise time constant were observed for Arg-82 mutants of bR (e.g., an approximately 10-times increase of R82A^{bR}) (Balashov et al., 1993; Hatanaka et al., 1996).

Effect on the M-decay rate

Fig. 3 shows the traces of flash-photolysis data (in 400 mM NaCl, pH 8.0) at selected wavelengths for the wild-type and various Arg-72 mutants of *p*pR. Clearly, Arg-72 mutants of *p*pR show much faster M-decay than the wild-type depending on mutants. The M-decay was analyzed by a single exponential equation, and the rate constants for various mutants of *p*pR were 1.7, 45.3, 14.3, 10.4, and 40.8 s^{-1} for the wild-type, R72A, R72K, R72Q, and R72S, respectively. As a result of the fast M-decay, the O-intermediate shows a faster rise with a larger amplitude, but the decay rate of the O-intermediate or the recovery rate of the original pigment is scarcely changed.

R72A/D193N double mutant shows slow M-decay

Fig. 4 shows flash-photolysis data at typical wavelengths for the R72A/D193N^{ppR} (*left*) and R72A/D193E^{ppR} double

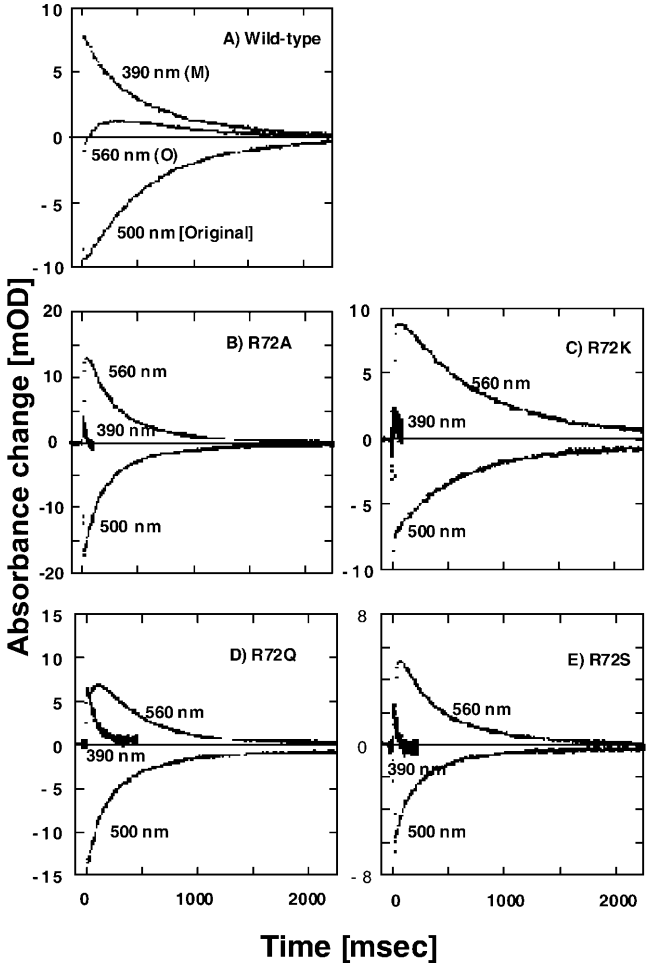

FIGURE 3 Flash-photolysis data of selected wavelengths for the wild-type (*A*), R72A^{ppR} (*B*), R72K^{ppR} (*C*), R72Q^{ppR} (*D*), and R72S^{ppR} (*E*). All samples were reconstituted with egg-PC. Absorbance changes in 390, 500, and 560 nm monitor the concentration of M-intermediate, *p*R, and O-intermediate, respectively. The medium was 400 mM NaCl buffered with 10 mM of MES plus CHES at pH 8.0. Temperature was 20°C.

mutants (*right*). It is very interesting that in contrast to the R72A^{ppR} single mutant, R72A/D193N^{ppR} shows that M-decay is approximately two times slower than that of the wild-type (Fig. 3 *A*). On the other hand, R72A/D193E^{ppR} shows very fast M-decay, which is the same as for the R72A single mutant.

M-decay rate of mutants-mutants under varying pH

The M-decay rates of various Arg-72^{ppR} mutants of *p*pR were measured under varying pH. The results are plotted in Fig. 5 where the ordinate represents the logarithm of the M-decay rate constant, k_1 (s^{-1}). The mutants are R72A (■), R72K (◆), R72Q (▲), R72S (▼), R72A/D193N (□) and R72A/D193E (◪), and the data for the wild-type are shown by ○. This figure reveals that log k_1 is approximately linear with pH for all Arg-72^{ppR} mutants except for R72A/D193N

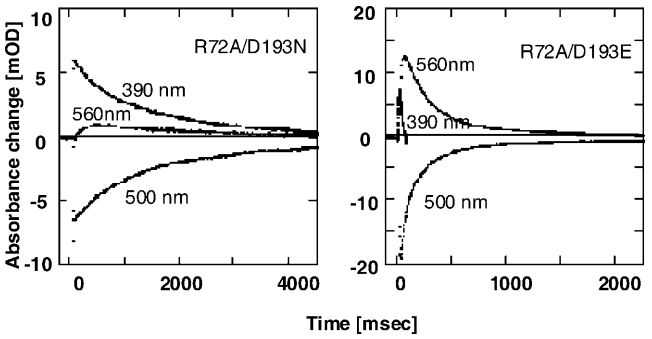

FIGURE 4 Flash-photolysis data of selected wavelengths for R72A/D193N (*left*) and R72A/D193E (*right*) *p*pR mutants. Experimental conditions were the same as in Fig. 3.

and the wild-type. The slopes of these Arg mutants are 0.74 (R72A), 0.96 (R72K), 0.88 (R72Q), 0.58 (R72S), and 0.79 (R72A/D193E), indicating that the slope is close to unity except for R72S. For this mutant, relatively larger values are obtained in the pH range from 8.8 to 9.5; the reason for this is not known. If these are omitted for the regression, the slope will become larger.

In Fig. 1, the pH-titration profile of $R72K^{ppR}$ is different from that of the other Arg-mutants whereas the pH profiles of mutants shown in Fig. 5 are all similar. Perhaps this is because the lysine residue is in its neutral form under the condition of Fig. 5 (pH 7.5–10), but bears a positive charge under the conditions of Fig. 1 (pH $<$ 7).

Photoinduced proton pumping activity of Arg-72^{ppR} mutants

The process of M-decay involves the protonation of the deprotonated Schiff base. The proton-donating residue of bR, Asp-96, is replaced with Phe-86 in *p*pR (Seidel et al., 1995); the cytoplasmic channel (CP) of *p*pR, then, is very hydrophobic—suggesting that the proton conductivity through the CP is very small. Nevertheless, light-induced proton pumping is observed for *p*pR alone, implying that proton transfer through CP occurs during M-decay. On the other hand, complex formation of *p*pR with *p*HtrII stops the light-induced proton pumping with little or no change in the M-decay rate (Sudo et al., 2001; Schmies et al., 2001; Hippler-Mreyen et al., 2003). This has been interpreted as follows: Association with *p*HtrII results in the closure of the CP channel, and hence, for the complex, the proton should come to the deprotonated Schiff base solely through EC, implying no proton pumping activity of the complex. For *p*pR alone, the ratio of the proton conductivity of EC/CP might be large and then the M-decay rate of *p*pR might be unchanged by its association with *p*HtrII despite the CP-channel closure. The proton is released to EC and taken up both from EC and CP during photocycling. Therefore, the proton uptake via EC is futile for the photoinduced proton pumping of *p*pR, and the photoinduced proton pumping activity of *p*pR alone is a rough measure for the fraction of the proton entry from CP to the deprotonated Schiff base.

Results of light-induced proton pumping experiments with inside-out membrane vesicles containing various Arg-72^{ppR} mutants are shown in Fig. 6. The amount of pigment was kept constant for all mutants (66 μg). No light-induced proton movements were observed for the membrane vesicles derived from cells containing the vector alone, which did not express *p*pR (data not shown). In Fig. 6, two corrections have been made to account for two distortions of the data. The first correction is for the fraction of the bathochromic pink form that is unable to pump protons due to the protonation of the counterion of Schiff base, Asp-75^{ppR}, in the dark. This fraction was estimated from the pK_a values shown in Fig. 1. The second correction is for the turnover rate; the amounts of protons transported per unit time should be proportional to the rate, which was estimated from the half-time of the recovery to the original pigment. The activity of R72A/

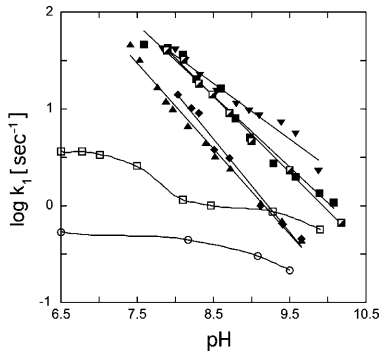

FIGURE 5 The logarithm of k_1, the rate constant of the M-decay, is plotted against pH in the medium. The mutants are R72A (■), R72K (♦), R72Q (▲), R72S (▼), R72A/D193N (□), and R72A/D193E (◪), and data of the wild-type are shown by ○. Experimental conditions were the same as in Fig. 3.

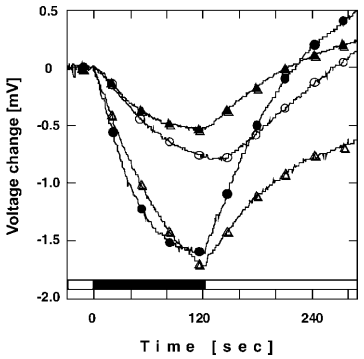

FIGURE 6 Photoinduced proton-pumping through inside-out membrane vesicles derived from *E. coli* cells expressing *p*pR or mutants. Data were corrected by two factors (for details, see Results). ●, the wild-type; ○, R72A; ▲, R72A/D193E; and △, R72A/D193N. The medium contained 400 mM NaCl at pH 6.5 without buffer.

D193N^{ppR} is almost equal to that of the wild-type (~80%), and R72A^{ppR} and R72A/D193E^{ppR} show ~30% of the activity of the wild-type. It is interesting that the mutants having the faster M-decay have lower activity than those having the slower M-decay.

DISCUSSION

Assignment of the residue *X*

Results of Fig. 1 reveal that the positive charge at the Arg-72^{ppR} position decreases the pK_a of Asp-75^{ppR}, the counterion of the Schiff base. Similar observations have been reported for bR. The pK_a of the counterion for R82A^{bR} and R82Q^{bR} was increased to ~7 whereas that of the wild-type was 2.5, and the replacement by the positively charged residue (R82K^{bR}) kept the pK_a at a relatively low value of 3.5 (Balashov et al., 1995). The magnitudes of pK_a changes in *p*pR caused by the replacement with the neutral amino acids are smaller than those of bR, however. This may be because of the difference in the direction of the guanidinium pointing toward the Schiff base in bR or pointing away from the Schiff base in *p*pR, which increases the distance between the positive charge and the counterion in bR (Luecke et al., 2001; Royant et al., 2001).

As described in Results, the residue *X* is required for quantitative explanations for Fig. 1 (see the inset). What is the residue *X*? Since Asp-75^{ppR} is deprotonated in the dark at neutral pH, the pK_a of the residue *X* may be 5.7, that is, the pK_{a2} value of the wild-type. The residue *X* might be Asp-193^{ppR}. Reasons for this assignment: it has been shown that pK_a of the counterion (Asp-85^{bR}) in bR is affected by the protonation state of Glu-204^{bR} (Richter et al., 1996; Govindjee et al., 1996) that corresponds to Asp-193^{ppR}. In addition, we showed previously that the electric charge of residue 193 of *p*pR affects the pK_a of the Schiff base (Iwamoto et al., 2002a), indicating that Asp-75^{ppR}, Arg-72^{ppR}, and Asp-193^{ppR} are connected via hydrogen-bonding through water molecules as is shown in x-ray crystal structure (Pebay-Peyroula et al., 2002).

Light-induced proton transfer reactions on the wild-type and Arg-72^{ppR}

Fig. 2 shows the difference between the order of the flash-induced proton release and uptake between the wild-type and Arg-72^{ppR}. Iwamoto et al. (2004) showed that light-induced proton release at the earlier stage of the photocycling was not observed for D193N^{ppR} under the present conditions, suggesting strongly that Asp-193^{ppR} is a key residue involved in proton release. Note that Asp-193^{ppR} corresponds to Glu-204^{bR}, which is one of the members of the proton-releasing complex in bR (Balashov et al., 1997; Dioumaev et al., 1998; Koyama et al., 1998).

In bR, the movement of the orientation of the side chain of Arg-82^{bR} during photocycling is considered to cause a pK_a change of the proton-releasing complex consisting of Glu-194^{bR} and Glu-204^{bR} (Tanio et al., 1999; Petkova et al., 1999; Royant et al., 2000; Luecke et al., 1999; Luecke, 2000; Neutze et al., 2002). Therefore, the pK_a change in a group analogous to Glu-204^{bR}, the proton-releasing Asp-193^{ppR}, and the role of Arg-72^{ppR} in wild-type *p*pR, are very interesting. So far we have no information concerning the possible movement of Arg-72^{ppR} during photocycle.

At the pH where the first proton release is observed from the wild-type, Asp-193^{ppR} may be protonated, and then proton transfer from the Schiff base to deprotonated Asp-75^{ppR} leads to the proton release from the protonated Asp-193^{ppR}. A proton absorbed after release is used for the protonation of the Schiff base and the deprotonated Asp-193^{ppR} is reprotonated with the proton from Asp-75^{ppR} during O-decay. Above pH 7, Asp-193^{ppR} may be deprotonated, presumably for the earlier intermediates and certainly at the *p*pR ground state (pKa ~5.7) so that the first proton release cannot be induced. The decrease in the signal (its absolute magnitude) above pH 9 might be caused by the slowing-down of the proton-uptake rate due to high pH in the medium. Below pH 4.5, why does the proton uptake first occur even though Asp-193^{ppR} may be protonated? The proton concentration in the external medium might be so high that the proton cannot be released from Asp-193^{ppR}, resulting in the first proton uptake followed by the slow release.

In contrast to the wild-type, R72A^{ppR} shows first light-induced proton uptake over the whole pH range, followed by release. Thus, for the Arg-mutant, it seems that the proton transfer from the Schiff base to Asp-75^{ppR} cannot be ''transmitted'' to Asp-193^{ppR}, a proton-releasing residue, due to the lack of the arginine residue. The proton now on Asp-75^{ppR} may be used for the reprotonation of the Schiff base; if so, the proton that is released may be from the deprotonation of Asp-75^{ppR}.

M-decay of Arg-72^{ppR}

A remarkable observation from Fig. 3 is that the M-decay of Arg-72^{ppR} mutants is faster than that of the wild-type. As postulated previously (Sudo et al., 2001), the proton that reprotonates the deprotonated Schiff base at the M-decay comes from both the CP and EC sides, and due to the hydrophobic nature of CP, the main route may be the one through the EC domain. Therefore, we conclude that Arg-72^{ppR}, located in EC, hinders proton transfer through the EC to the deprotonated Schiff base at M-decay. This in turn prolongs the lifetime of the M-intermediate of the wild-type, one of signaling states for phototaxis (Yan et al., 1991).

Fig. 4 shows the slow M-decay of R72A/D193N^{ppR} in sharp contrast to those of R72A/D193E^{ppR} and the Arg-72^{ppR} single mutants (Fig. 3). This result implies that, for R72A^{ppR} and presumably all Arg-72^{ppR} mutants, proton uptake from the EC side is mediated or controlled by Asp-193^{ppR}—which is located nearly at the end of EC, open to

the external medium. We note that log k_1 is approximately a linear function of pH in the region of ~7.5–9. This may be interpreted as the passive proton transport through EC of Arg-72^{ppR}. Another possible interpretation is that the proton transfer at M-decay of Arg-72^{ppR} is mediated by the protonated Asp-193^{ppR}. In this pH range, the Henderson-Hasselbalch equation predicts that the slope should be −1 when the logarithm of the fraction of protonated carboxyl group is plotted against pH, because the pK_a of Asp-193^{ppR} is probably far lower than the pH investigated (5.7 at the *p*pR ground state; pK_a values for the intermediates are not known). A further interesting problem is whether Asp-193 of the wild-type *p*pR also controls the proton transfer through EC. Studies are now in progress using D193N^{ppR}.

Proton-pumping activity

Fig. 6 shows that the mutants having faster M-decay have lower light-induced proton-pumping activity compared to the wild-type. If we accept the concept that the increase in the M-decay rate of Arg-72^{ppR} mutants is due to the increase in the proton transfer through EC and that this proton pathway does not contribute the proton-pumping, the results of Fig. 6 are qualitatively conceivable. At pH = 8, the M-decay rate constant of the wild-type is 1.7 s^{-1} whereas that of R72A^{ppR} is 45.3 s^{-1}, indicating that, in the mutant, almost all protons that cause the reprotonation of the Schiff base during the M-decay are from the EC. This would predict that the proton-pumping activity might be more reduced than that observed. Therefore, we would have to consider other factors that control the light-induced proton pumping activity. One possibility is a two-photon process which was hypothesized originally to account for the unexpected strong proton-pumping of the wild-type in the presence of azide (Schmies et al., 2000), in which the O-intermediate was accumulated due to the fast M-decay, similar to the present experiment. The photoreactivity of the O-intermediate increases the turnover rate of the pigment under continuous illumination. Iwamoto et al. (2002b) verified the photoreactivity. A second possibility is an increase in the proton conductivity in the CP caused by the mutation of the arginine residue even though it is located in EC. The last possibility is that there might be two M-states, as in bR (Lanyi and Schobert, 2003), and only one contributes to the proton-pumping (M2 as is in bR). We should take into consideration the transition from M1 to M2, or the population of these two M-states being affected by the mutation. The spectroscopically separated two-M-states of the wild-type *p*pR was described in Chizhov et al. (1998) and Rivas et al. (2003). Further quantitative study on this respect should be necessary.

Effect on the chloride concentration in the medium

The Cl^- effect on characteristics and photochemistry of *p*pR has been reported (Iwamoto et al., 2002a; Shimono et al., 2000). In addition, we observed here a Cl^- effect on M-decay rate of R72A^{ppR} (Fig. 7). As discussed above, this result may indicate a Cl^- effect on the pK_a of Asp-193^{ppR} of R72A. The Cl^- concentration we used here was only 400 mM NaCl.

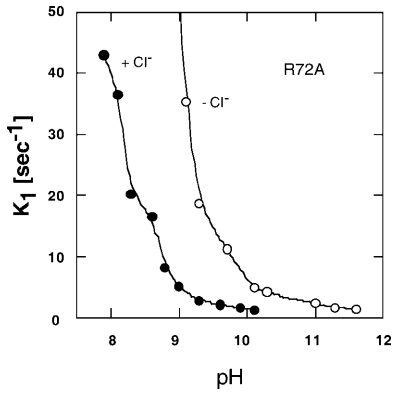

FIGURE 7 Cl^- concentration dependence of the M-decay rate constant of R72A^{ppR}. ● shows the data in the presence of 400 mM NaCl and the ○ shows the data in the absence of Cl^-. The medium was buffered with 10 mM MES plus CHES at pH 8.

CONCLUDING REMARKS

In this article, we conclude the following:

1. Arg-72^{ppR} decreases the pK_a of Asp-75^{ppR}, the counter-ion of the protonated Schiff base.
2. Replacement of Arg-72^{ppR} increases the M-decay rate, which may be the result of increased proton transfer rate through the EC. In other words, Arg-72^{ppR} in the wild-type prevents this proton transfer, leading to the prolongation of the lifetime of M-intermediate; the effect is enhanced by lack of a proton-donating residue at the Asp-96^{bR} position (Iwamoto et al., 1999b).
3. Substitution for the arginine residue at position 72 changes the timing of proton release and uptake from that of the wild-type. The lack of the arginine residue may disconnect the intramolecular proton transfer chain from the Schiff base and the extracellular part.

Further investigation on the role of Arg-72^{ppR} on proton transfer will be of interest. One reason for its behavior may be that the orientation of the guanidinium in the dark is opposite to that of bR; we do not yet know whether this guanidinium group of Arg-72 moves to change the distance from Asp-193 during photocycling as bR.

The authors thank Sergei Balashov and Hideki Kandori for their invaluable discussions, and Takashi Kikukawa and Tsunehisa Araiso for permission to use their laser flash-photolysis apparatus.

This work was supported by Grants-in-Aid for Scientific Research from the Japanese Ministry of Education, Science, Sports and Culture.

REFERENCES

Balashov, S. P., E. S. Imasheva, T. G. Ebrey, N. Chen, D. R. Menick, and R. K. Crouch. 1997. Glutamate 194 to cysteine mutation inhibits fast light-induced proton release in bacteriorhodopsin. *Biochemistry.* 36: 8671–8676.

Balashov, S. P., R. Govindjee, E. Imasheva, S. Misra, T. G. Ebrey, Y. Feng, R. K. Crouch, and D. R. Menick. 1995. The two pK_a of aspartate 85 and control of thermal summarization and proton release in the arginine 82 to lysine mutant of bacteriorhodopsin. *Biochemistry.* 34:8820–8834.

Balashov, S. P., R. Govindjee, M. Kono, E. Imasheva, E. Lukashev, T. G. Ebrey, R. K. Crouch, D. R. Menick, and Y. Feng. 1993. Effect of the arginine 82 to alanine mutation in bacteriorhodopsin on dark-adaptation, proton release, and the photochemical cycle. *Biochemistry.* 32:10331–10343.

Beja, O., E. N. Spudich, J. L. Spudich, M. Leclerc, and E. F. DeLong. 2001. Proteorhodopsin phototrophy in the ocean. *Nature*. 411:786–789.

Bieszke, J. A., E. L. Braun, L. E. Bean, S. C. Kang, D. O. Natvig, and K. A. Borkovich. 1999. The NOP-1 gene of *Neurospora crassa* encodes a seven-transmembrane helix retinal-binding protein homologous to archaeal rhodopsins. *Proc. Natl. Acad. Sci. USA*. 96:8034–8039.

Brown, L. S. 2001. Proton transport mechanism of bacteriorhodopsin as revealed by site-specific mutagenesis and protein sequence variability. *Biochem. Moscow*. 66:1249–1255.

Chizhov, I., G. Schmies, R. Seidel, J. R. Sydor, B. Luttenberg, and M. Engelhard. 1998. The photophobic receptor from *Natronobacterium pharaonis*: temperature and pH dependencies of the photocycle of sensory rhodopsin II. *Biophys. J.* 75:999–1009.

Dioumaev, A. K., H. T. Richter, L. S. Brown, M. Tanio, S. Tuzi, H. Saito, Y. Kimura, R. Needleman, and J. K. Lanyi. 1998. Existence of a proton transfer chain in bacteriorhodopsin: participation of Glu-194 in the release of protons to the extracellular surface. *Biochemistry.* 37:2496–2509.

Gordeliy, V. I., J. Labahn, R. Moukhametzianov, R. Efremov, J. Granzin, R. Schlesinger, G. Büldt, T. Savopol, A. J. Scheidig, J. P. Klare, and M. Engelhard. 2002. Molecular basis of transmembrane signaling by sensory rhodopsin II-transducer complex. *Nature.* 419:484–487.

Govindjee, R., S. Misra, S. P. Balashov, T. G. Ebrey, R. K. Crouch, and D. R. Menick. 1996. Arginine 82 regulates the pK_a of the group responsible for the light-driven proton release in bacteriorhodopsin. *Biophys. J.* 71: 1011–1023.

Haupts, U., J. Tittor, and D. Oesterhelt. 1999. Closing in on bacteriorhodopsin: progress in understanding the molecule. *Annu. Rev. Biophys. Biomol. Struct.* 28:367–399.

Hatanaka, M., J. Sasaki, H. Kandori, T. G. Ebrey, R. Needleman, J. K. Lanyi, and A. Maeda. 1996. Effects of arginine 82 on the interactions of internal water molecules in bacteriorhodopsin. *Biochemistry.* 35:6308–6312.

Hippler-Mreyen, S., J. P. Klare, A. A. Wegener, R. Seidel, C. Herrmann, G. Schmies, G. Nagel, G. E. Bamberg, and M. Engelhard. 2003. Probing the sensory rhodopsin II binding domain of its cognate transducer by calorimetry and electrophysiology. *J. Mol. Biol.* 330:1203–1213.

Hirayama, J., Y. Imamoto, Y. Shichida, N. Kamo, H. Tomioka, and T. Yoshizawa. 1992. A photocycle of phoborhodopsin from haloalkaliphilic bacterium (*Natronobacterium pharaonis*) studied by low-temperature spectrophotometry. *Biochemistry.* 31:2093–2098.

Hoff, W. D., K.-H. Jung, and J. L. Spudich. 1997. Molecular mechanism of photosignaling by archaeal sensory rhodopsins. *Annu. Rev. Biophys. Biomol. Struct.* 26:223–258.

Ihara, K., T. Umemura, I. Katagiri, T. Kitagima-Ihara, Y. Sugiyama, Y. Kimura, and Y. Mukohata. 1999. Evolution of the archaeal rhodopsins: evolution rate changes by gene duplication and functional differentiation. *J. Mol. Biol.* 285:163–174.

Ikeura, Y., K. Shimono, M. Iwamoto, Y. Sudo, and N. Kamo. 2003. Arg-72 of *pharaonis* phoborhodopsin (sensory rhodopsin II) is important for the maintenance of the protein structure in the solubilized state. *Photochem. Photobiol.* 77:96–100.

Ikeura, Y., K. Shimono, M. Iwamoto, Y. Sudo, and N. Kamo. 2002. Influence of Arg72 of *pharaonis* phoborhodopsin on M-intermediate decay and proton pumping activity. *J. Photosci.* 9:311–313.

Imamoto, Y., Y. Shichida, J. Hirayama, H. Tomioka, N. Kamo, and T. Yoshizawa. 1992a. Chromophore configuration of *pharaonis* phoborhodopsin and its isomerization on photon absorption. *Biochemistry.* 31: 2523–2528.

Imamoto, Y., Y. Shichida, J. Hirayama, H. Tomioka, N. Kamo, and T. Yoshizawa. 1992b. Nanosecond laser photolysis of phoborhodopsin from *Natronobacterium pharaonis*: appearance of KL- and L-intermediates in the photocycle at room temperature. *Photochem. Photobiol.* 56:1129–1134.

Iwamoto, M., C. Hasegawa, Y. Sudo, K. Shimono, T. Araiso, and N. Kamo. 2004. Proton release and uptake of *pharaonis* phoborhodopsin (sensoryrhodopsin II) reconstituted into phospholipids. *Biochemistry.* 43:3195–3203.

Iwamoto, M., Y. Furutani, N. Kamo, and H. Kandori. 2003. Proton transfer reactions in the F86D and F86E mutants of *pharaonis* phoborhodopsin (sensory rhodopsin II). *Biochemistry.* 42:2790–2796.

Iwamoto, M., Y. Furutani, Y. Sudo, K. Shimono, H. Kandori, and N. Kamo. 2002a. Role of Asp^{193} in chromophore-protein interaction of *pharaonis* phoborhodopsin (sensory rhodopsin II). *Biophys. J.* 83:1130–1135.

Iwamoto, M., Y. Sudo, K. Shimono, and N. Kamo. 2002b. Illumination accelerates the decay of the O-intermediate of *pharaonis* phoborhodopsin (sensory rhodopsin II). *Photochem. Photobiol.* 76:462–466.

Iwamoto, M., K. Shimono, M. Sumi, K. Koyama, and N. Kamo. 1999a. Light-induced proton uptake and release of *pharaonis* phoborhodopsin detected by a photoelectrochemical cell. *J. Phys. Chem. B.* 103:10311–10315.

Iwamoto, M., K. Shimono, M. Sumi, and N. Kamo. 1999b. Positioning proton-donating residues to the Schiff base accelerates the M-decay of *pharaonis* phoborhodopsin expressed in *Escherichia coli*. *Biophys. Chem.* 79:187–192.

Jung, K. H., V. D. Trivedi, and J. L. Spudich. 2003. Demonstration of a sensory rhodopsin in eubacteria. *Mol. Microbiol.* 47:1513–1522.

Kamo, N., K. Shimono, M. Iwamoto, and Y. Sudo. 2001. Photochemistry and photoinduced proton-transfer by *pharaonis* phoborhodopsin. *Biochem. Moscow.* 66:1277–1282.

Kandori, H., K. Shimono, Y. Sudo, M. Iwamoto, Y. Shichida, and N. Kamo. 2001. Structural changes of *pharaonis* phoborhodopsin upon photoisomerization of the retinal chromophore: infrared spectral comparison with bacteriorhodopsin. *Biochemistry.* 40:9238–9246.

Kolbe, M., H. Besir, L. O. Essen, and D. Oesterhelt. 2000. Structure of the light-driven chloride pump halorhodopsin at 1.8 Ångstrom resolution. *Science.* 288:1390–1396.

Koyama, K., T. Miyasaka, R. Needleman, and J. K. Lanyi. 1998. Photoelectrochemical verification of proton-releasing groups in bacteriorhodopsin. *Photochem. Photobiol.* 68:400–406.

Lanyi, J. K., and B. Schobert. 2003. Mechanism of proton transport in bacteriorhodopsin from crystallographic structures of the K, L, M1, M2, and M2′ intermediates of the photocycle. *J. Mol. Biol.* 328:439–450.

Lanyi, J. K., and H. Luecke. 2001. Bacteriorhodopsin. *Curr. Opin. Struct. Biol.* 11:415–419.

Luecke, H., B. Schobert, J. K. Lanyi, E. N. Spudich, and J. L. Spudich. 2001. Crystal structure of sensory rhodopsin II at 2.4 Å: insights into color tuning and transducer interaction. *Science.* 293:1499–1503.

Luecke, H. 2000. Atomic resolution structures of bacteriorhodopsin photocycle intermediates: the role of discrete water molecules in the function of this light-driven ion pump. *Biochim. Biophys. Acta.* 1460:133–156.

Luecke, H., B. Schobert, H. T. Richter, J. P. Cartailler, and J. K. Lanyi. 1999. Structural changes in bacteriorhodopsin during ion transport at 2 Ångstrom resolution. *Science.* 286:255–260.

Lüttenberg, B., E. K. Wolff, and M. Engelhard. 1998. Heterologous coexpression of the blue light receptor psRII and its transducer pHtrII

from *Natronobacterium pharaonis* in the *Halobacterium salinarum* strain Pho^{81}/w restores negative phototaxis. *FEBS Lett*. 426:117–120.

Miyazaki, M., J. Hirayama, M. Hayakawa, and N. Kamo. 1992. Flash photolysis study on *pharaonis* phoborhodopsin from a haloalkaliphilic bacterium (*Natronobacterium pharaonis*). *Biochim. Biophys. Acta*. 1140:22–29.

Mukohata, Y., K. Ihara, T. Tamura, and Y. Sugiyama. 1999. Halobacterial rhodopsins. *J. Biochem*. 125:649–657.

Neutze, R., E. Pebay-Peyroula, K. Edman, A. Royant, J. Navarro, and E. M. Landau. 2002. Bacteriorhodopsin: a high-resolution structural view of vectorial proton transport. *Biochim. Biophys. Acta*. 1565:144–167.

Pebay-Peyroula, E., A. Royant, E. M. Landau, and J. Navarro. 2002. Structural basis for sensory rhodopsin function. *Biochim. Biophys. Acta*. 1565:196–205.

Oesterhelt, D., and W. Stoeckenius. 1971. Rhodopsin-like protein from the purple membrane of *Halobacterium halobium*. *Nat. New Biol*. 233: 149–152.

Petkova, A. T., J. G. G. Hu, M. Bizounok, M. Simpson, R. G. Griffin, and J. Herzfeld. 1999. Arginine activity in the proton-motive photocycle of bacteriorhodopsin: solid-state NMR studies of the wild-type and D85N proteins. *Biochemistry*. 38:1562–1572.

Richter, H. T., L. S. Brown, R. Needleman, and J. K. Lanyi. 1996. A linkage of the pK_as of Asp-85 and Glu-204 forms part of the reprotonation switch of bacteriorhodopsin. *Biochemistry*. 35:4054–4062.sd

Rivas, L., S. Hippler-Mreyen, M. Engelhard, and P. Hildebrandt. 2003. Electric-field dependent decays of two spectroscopically different M-states of photosensory rhodopsin II from *Natronobacterium pharaonis*. *Biophys. J*. 84:3864–3873.

Royant, A., P. Nollert, K. Edman, R. Neutze, E. M. Landau, E. Pebay-Peyroula, and J. Navarro. 2001. X-ray structure of sensory rhodopsin II at 2.1 Å resolution. *Proc. Natl. Acad. Sci. USA*. 98:10131–10136.

Royant, A., K. Edman, T. Ursby, E. Pebay-Peyroula, E. M. Landau, and R. Neutze. 2000. Helix deformation is coupled to vectorial proton transport in the photocycle of bacteriorhodopsin. *Nature*. 406:645–648.

Sasaki, J., and J. K. Spudich. 2000. Proton transport by sensory rhodopsins and its modulation by transducer-binding. *Biochim. Biophys. Acta*. 1460:230–239.

Scharf, B., B. Pevec, B. Hess, and M. Engelhard. 1992. Biochemical and photochemical properties of the photophobic receptors from *Halobacterium halobium* and *Natronobacterium pharaonis*. *Eur. J. Biochem*. 206:356–366.

Schmies, G., M. Engelhard, P. G. Wood, G. Nagel, and E. Bamberg. 2001. Electrophysiological characterization of specific interactions between bacterial sensory rhodopsins and their transducers. *Proc. Natl. Acad. Sci. USA*. 98:1555–1559.

Schmies, G., B. Luttenberg, I. Chizhov, M. Engelhard, A. Becker, and E. Banburg. 2000. Sensory rhodopsin II from the haloalkaliphilic *Natronobacterium pharaonis*: light-activated proton transfer reactions. *Biophys. J*. 78:967–976.

Seidel, R., B. Scharf, M. Gautel, K. Kleine, D. Oesterhelt, and M. Engelhard. 1995. The primary structure of sensory rhodopsin II: a membrane of an additional retinal protein subgroup is coexpressed with its transducer, the halobacterial transducer of rhodopsin II. *Proc. Natl. Acad. Sci. USA*. 92:3036–3040.

Shimono, K., M. Kitami, M. Iwamoto, and N. Kamo. 2000. Involvement of two groups in reversal of the bathochromic shift of *pharaonis* phoborhodopsin by chloride at low pH. *Biophys. Chem*. 87:225–230.

Shimono, K., M. Iwamoto, M. Sumi, and N. Kamo. 1998. V108 mutant of *pharaonis* phoborhodopsin: substitution caused no absorption change but affected its M-state. *J. Biochem*. 124:404–409.

Shimono, K., M. Iwamoto, M. Sumi, and N. Kamo. 1997. Functional expression of *pharaonis* phoborhodopsin in *Escherichia coli*. *FEBS Lett*. 420:54–56.

Sineshchekov, O. A., K. H. Jung, and J. L. Spudich. 2002. Two rhodopsins mediate phototaxis to low- and high-intensity light in *Chlamydomonas reinhardtii*. *Proc. Natl. Acad. Sci. USA*. 99:8689–8694.

Spudich, J. L., C.-S. Yang, K.-H. Jung, and E. N. Spudich. 2000. Retinylidene proteins: structures and functions from archaea to humans. *Annu. Rev. Cell Dev. Biol*. 16:365–392.

Spudich, J. L. 1998. Variations on a molecular switch-transport and sensory signaling by archaeal rhodopsins. *Mol. Microbiol*. 28:1051–1058.

Spudich, J. L., and R. A. Bogomolni. 1984. Mechanism of colour discrimination by a bacterial sensory rhodopsin. *Nature*. 312:509–513.

Sudo, Y., M. Iwamoto, K. Shimono, M. Sumi, and N. Kamo. 2001. Photo-induced proton transport of *pharaonis* phoborhodopsin (sensory rhodopsin II) is ceased by association with the transducer. *Biophys. J*. 80:916–922.

Takahashi, T., H. Tomioka, N. Kamo, and Y. Kobatake. 1985. A photosystem other than PS370 also mediates the negative phototaxis of *Halobacterium halobium*. *FEMS Microbiol. Lett*. 28:161–164.

Tanio, M., S. Tuzi, S. Yamaguchi, R. Kawaminami, A. Naito, R. Needleman, J. K. Lanyi, and H. Saito. 1999. Conformational changes of bacteriorhodopsin along the proton-conduction chain as studied with C-13 NMR of [3-C-13]-Ala-labeled protein: Arg^{82} may function as an information mediator. *Biophys. J*. 77:1577–1584.

Tomioka, H., T. Takahashi, N. Kamo, and Y. Kobatake. 1986. Action spectrum of the photoattractant response of *Halobacterium halobium* in early logarithmic growth phase and the role of sensory rhodopsin. *Biochim. Biophys. Acta*. 884:578–584.

Varo, G. 2000. Analogies between halorhodopsin and bacteriorhodopsin. *Biochim. Biophys. Acta*. 1460:220–229.

Yan, B., T. Takahashi, R. Johnson, and J. L. Spudich. 1991. Identification of signaling states of a sensory receptor by modulation of lifetimes of stimulus-induced conformations: the case of sensory rhodopsin II. *Biochemistry*. 30:10686–10692.

Yang, C. S., and J. L. Spudich. 2001. Light-induced structural changes occur in the transmembrane helices of the *Natronobacterium pharaonis* HtrII transducer. *Biochemistry*. 40:14207–14214.

Yao, V. J., and J. L. Spudich. 1992. Primary structure of an archaebacterial transducer, a methyl-accepting protein associated with sensory rhodopsin I. *Proc. Natl. Acad. Sci. USA*. 89:11915–11919.

Zhang, X.-N., J. Zhu, and J. L. Spudich. 1999. The specificity of interaction of archaeal transducers with their cognate sensory rhodopsin is determined by their transmembrane helices. *Proc. Natl. Acad. Sci. USA*. 96:857–862.